# Mathematical Model to Predict Nitric Oxide Equilibrium Concentration in a Direct Injection Diesel Engine: Part-III

Ramendra Singh Niranjan, Department of Mechanical Engineering, UIET, CSJM University Kanpur, 208024, India
Bristi Mitra, Department of Chemical Engineering, UIET, CSJM University Kanpur, 208024, India
Rajesh Kumar Prasad*, Department of Mechanical Engineering,, ICFAI University Jharkhand, Ranchi-835222, India
*Corresponding Author:rajeshpd2010@gmail.com

## Abstract

Euro VI/BS VI emission norms, limited emissions prediction models forces researchers to think about to develop a numerical model which actively predict and control chemical kinetics emission species during combustion phase to reduce the cost associated with after-treatment systems. This study is focused on the simulation and experimental investigation of simplified model for prediction of species concentration especially atomic oxygen [O], Nitrogen [$N_2$] and nitric oxide [NO]. Burned flame temperature and thermal NO concentrations were simulated by enthalpy balance and Zeldovich mechanism respectively. The simulated results were validated with experimental result of Turbocharged direct injected Diesel engine at steady-state operating conditions of 2200 rpm and 1400 rpm with varying load. The maximum temperature ($T_{max}$) simulated within burned zone at 2200 rpm &100% load is 2917K while at 75% load, and 50% load it reduces to 2853K, and 2776K respectively. It was also observed that the equilibrium concentrations of [O], [NO] and [$N_2$] were directly proportional to burned zone temperature. The accuracy of proposed model was tested at 2200 rpm and 1400 rpm with varying load such as full load, 75% load, and 50% load.

**Keywords: Burned zone temperature, Adiabatic flame temperature, $NO_x$ emissions, Zeldovich mechanism, DI diesel engine.**

## Introduction

Diesel engines are emitting more pollutant compared to gasoline engines but widely used due to higher power to weight ratio. It is most fuel efficient engines [1] since long but emissions such as NOx and soot from these engines creates acid rain, global warming etc. To reduce environmental complication reliable pollutants prediction model needed to optimize the NOx vs soot trade off [2, 3]. In gasoline engine, NOx formation is major contributor to acid rain, ozone layer depletion and it is reduced by leaning the combustible mixture [4] while diesel combustion could be due to either thermal route or fuel bound or prompt formation route or via $N_2O$ route. In this work, only thermal NOx concentration prediction model was considered using Zeldovich mechanism [5-8] which is a temperature dependent phenomena [9]. In the past, few engine researchers proposed NOx prediction mathematical model with different operation variables [10], while few of them considered cyclic NOx evolution using the in-cylinder pressure (P) Vs crank angle (Ө) data as an input quantity [5,11,12]. The in-cylinder combustion pressure signal from pressure transducer provides details about combustion phasing, air flow rate [13], online fuel burning rate [14], misfire detection [15], control strategy of exhaust gas recirculation [16], engine torque estimation [17] and combustion noise control [18]. In this study, engine operating parameters along with engine specifications were noted to predict adiabatic flame temperature, and steady-state NOx concentration. Instantaneous NOx simulation models were developed with real time calculations [11, 12, 19]. All these proposed models combined with closed-loop control of few input parameters have a big potential on NOx reduction during combustion as well as in after-treatment [20, 21]. The zero-dimensional thermodynamic model is the simplest model which is based on empirical heat release model and predict NOx using time based ordinary differential equation while multi-dimensional CFD model is most complex which uses conservation of mass, energy and momentum and NOx prediction by solving partial differential equation which is the function of space and time [22].

Johansson et al, [23] developed NOx prediction model suitable for vehicle on-board, on-line implementation. A two-zone model, one burned zone in which the NOx formation takes place and one unburned zone composed of only air. After knowing the temperature of the burned zone, it was possible to compute the NO formation rate using the well-known 'Zeldovich mechanism'. Arsie et al, [24] developed a system of phenomenological models for

the simulation of combustion and NOx-Soot emissions of common-rail multi-jet Diesel engines. Andersson et al, [11] developed a fast NOx model which can be used for engine optimization, after treatment control or virtual mapping. A cylinder pressure was required as input data. High calculation speed was obtained by using table interpolation to calculate equilibrium temperatures and species concentrations.

### Experiments on 4-cylinder Engine

The first phase of experiments has been carried out on a 4-cylinder turbocharged DI Diesel engine. Diesel combustion was extensively studied by varying load at a speed of 2200 rpm and a BMEP of 8.6 bar by keeping constant injection timing. Intake manifold temperature was maintained at $105^0C$ by providing cooling system, and compression ratio of 17.5. The engine tests were done according to standard IS: 10000. Parameters like the speed of the engine, fuel and air flow rate, power, exhaust gas temperature, inlet air temperature and oil temperature were recorded and data has been used to compute other parameters. During the experiments every measurement was recorded average data of 30s at the end of 5 min stabilization of engine for every change of conditions.

Due to superior fuel economy and high power density direct injection Diesel engine have been widely used in heavy duty vehicles for a long time. In recent times this engine type has become more and popular for passenger cars, too, because improvements with respect to noise and vibration control have been achieved. However, due to increasingly strict international, national and other institutional legislations on engine emissions, more and more pressure is put on the research and development of diesel engine. Earlier design objectives were driven mainly by efficiency, reliability and durability. These items are now become secondary due to strict emission norms. Since control of NOx emissions dominates engine design practice. This can be achieved by detailed understanding of the chemical pathways for emission formation.

### Experimental Setup and Methodology

Figure 1 shows experimental setup of turbocharged diesel engine which is coupled with eddy current dynamometer. The engine specification remains identical as Part I & Part II [26, 27] is provided in Table 1.

Table 1: Engine specification

| Parameter | Specifications |
|---|---|
| Engine Model | 4- cylinder Turbocharged DI Diesel |
| Bore (mm)/ Stroke (mm) | 102/ 110 |
| Connecting rod length (mm) | 220 |
| IVC (CA)/ EVO (CA) | 210/ 540 |
| Rated speed (rpm) | 2200 |
| Compression ratio/ Swept volume (liter) | 17.4/ 0.9 per cylinder |
| Injection system | Common rail |

The engine suction side is fitted with all necessary accessories such as air-conditioning and measuring system, and fuel measuring unit while exhaust side is partially connected to emission analyzer. AVL Indiset, was used as data acquisition system during combustion.

Major pollutants emitted from the diesel engine exhaust are oxides of nitrogen (NOx), Smoke, Unburned Hydrocarbon (UHC) and Carbon-monoxides (CO). Exhaust gas analysis was done for all the species. For measurement of NOx, UHC and CO emissions, The chemiluminescence technique has been used to measure nitrogen oxides worldwide. Sample gas from engine exhaust was drawn into the analyzer and mixed with internally produced ozone. The following reaction takes place,

$$NO + O_3 \rightarrow NO_2^* + O_2 \qquad (1)$$
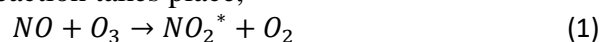
Only about 20% of the $NO_2$ goes into the excited state $NO_2^*$ in reaction [28]. This $NO_2^*$ reverts back to the ground state $NO_2$ while emitting electromagnetic radiation:

$$NO_2^* \rightarrow NO_2 + h_\vartheta \qquad (2)$$
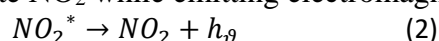
The radiation wave length range is in between 600-3000 nm and with an intensity maximum at approximately 1200 nm. When $O_3$ is present in excess, the signal is proportional to the NO concentration of the sample gas.
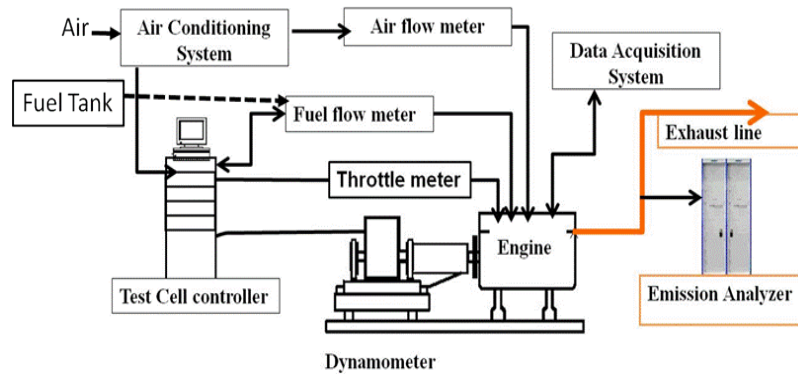


Fig.1. Engine experimental setup to collect data for validation of simulated results

The temperature at every crank angle can be determined by using the Ideal gas equation:

$$p\,V = mR\,T \tag{3}$$

### 4.3.7.1 Unburned Zone Temperature [11]

Unburned zone temperature can be calculated using the polytropic relation between temperature and pressure:

$$T_1 = T_0 \left(\frac{P_1}{P_0}\right)^{\frac{\gamma-1}{\gamma}} \tag{4}$$

### Burned zone temperature

Burned zone temperature before considering flame temperature can be calculated using isentropic relationship:

$$T_{exp,1} = T_{burn,0} \times \left(\frac{P_1}{P_0}\right)^{\frac{\gamma-1}{\gamma}} \tag{5}$$

Burned zone temperature after considering flame temperature is computed as:

$$T_{burn,1} = \left\{ T_{exp,1} \times m_{burn,0} + T_{flame,1} \times m_{flame,1} \right\}/\{m_{burn,1}\} \tag{6}$$

### Adiabatic Flame Temperature

The adiabatic flame temperature [25] of a steady-flow combustion process is determined by conventional assumption that the absolute enthalpy of a burned mixture element should equal the absolute enthalpy of an unburned mixture element, i.e.,

$$\sum_p N_i(h_{fo}+h_T - h_{298}) = \sum_R N_i(h_{fo}+h_T - h_{298}) \tag{7}$$

The assumption is made that the fuel is completely combusted into water and carbon dioxide.

### Chemical Kinetics of NOx

Besides particulate matter, nitrogen oxides are the most critical pollutants produced by diesel engines; they consist mostly of nitric oxide (or nitrogen monoxide) NO and nitrogen dioxide $NO_2$ (referred to, collectively, as NOx) with traces of di nitrogen trioxide $N_2O_3$ and di-nitrogen pentoxide $N_2O_5$. Nitrogen oxides are premixed phase of combustion, on the weak side of the reaction zone in the post-flame gases. Nitrogen oxides are highly active ozone precursors playing an important role in the smog chemistry. The principal reactions governing NO formation from molecular nitrogen and oxygen during combustion of lean or near stoichiometric fuel–air mixtures are usually described by the extended Zeldovich mechanism [25].

$$O+ N_2= NO+ N \tag{8}$$
$$N+ O_2= NO+ O \tag{9}$$
$$N+ OH= NO+ H \tag{10}$$

The third equation is considered only when the mixture is near Stoichiometric.

The rate constants selected by Bowman and Ragland from literature in units of $cm^3$/mol-s and temperature in K are given in table 2. The rate of formation of NO using the three reactions (8) to (10) can be expressed by the following equation;

$$\frac{d}{dt}[NO] = +k_1[O][N_2] - k_{-1}[NO][N] + k_2[N][O_2] - k_{-2}[NO][O] + k_3[N][OH] - k_{-3}[NO][H]$$

(11)

Where $k_1$, $k_2$ and $k_3$ are rate constants for the forward reactions (1), (2), and (3), respectively; subscript (-) denotes the rate constants for the reverse reactions, [ ] denotes the concentration of species in moles/cm$^3$.

Table 2 Reaction rates for NO formation mechanism, cm$^3$/mol-s, T in K

| Reaction | Forward | Reverse |
|---|---|---|
| $O+N_2=NO+N$ | $k_1=1.8 \times 10^{14} \times \exp(-38370/T)$ | $k_{-1}=3.8 \times 10^{13} \times \exp(-425/T)$ |
| $N+OH=NO+H$ | $k_2=1.8 \times 10^{10} \times \exp(-4680/T)$ | $k_{-2}=3.8 \times 10^{9} \times \exp(-20820/T)$ |
| $N+O_2=NO+O$ | $k_3=7.1 \times 10^{13} \times \exp(-450/T)$ | $k_{-3}=1.7 \times 10^{14} \times \exp(24560/T)$ |

To solve the equation (11) concentration of O$_2$, N$_2$, and radicals O, N, H, OH Are to be estimated. The dissociation of molecular N$_2$ is very small and the concentration of N$_2$ remains nearly constant. Further, two more assumptions as below are made:

(1) The concentrations of O, OH, O$_2$ and O are equilibrated.

Steady state assumption of [N] leads to,

$$\frac{d}{dt}[N] = +k_1[O][N_2] - k_{-1}[NO][N] - k_2[N][O_2] + k_{-2}[NO][O] - k_3[N][OH] + k_{-3}[NO][H] = 0$$

(12)

Use of equations (8) and (9) yield the rate of NO formation,

$$\frac{d}{dt}[NO] = 2\{k_1[O][N2] - k_{-1}[NO][N]\}$$

(13)

And from equation (9) steady state concentration of N,

$$[N]_{ss} = \frac{k_1[O][N] + k_{-2}[NO][O] + k_{-3}[NO][H]}{k_{-1}[NO] + k_2[O2] + k_3[OH]}$$

(14)

From the assumption of O, OH, H, and O$_2$,

$$\frac{[O_2][H]}{[O][OH]} = \frac{k_{-2} \cdot k_3}{k_2 \cdot k_{-3}}$$

Eliminating [N] and [H] gives,

$$\frac{d}{dt}[NO] = 2 k_1[O][N2] \frac{1 - \frac{[NO]^2}{k[O_2][N_2]}}{1 + \frac{k_{-1}[NO]}{k_2[O_2] + k_3[OH]}}$$

(15)

Where $K = (k_1 / k_{-1})(k_2 / k_{-2})$ is equilibrium constant for the reaction for the reaction

$$N_2 + O_2 \leftrightarrow 2NO$$

The NO formation rate may be calculated by equation (15) using equilibrium concentrations of O, O$_2$, OH and N$_2$. The rate of NO formation is much slower than the combustion rates. Most of NO formation takes place in the burned gases behind the flame front after the combustion is completed locally .The NO formation process can be decoupled from combustion process and the rate of formation of NO can be calculated assuming equilibrium values of concentrations of O, O$_2$, OH and N2. By introducing equilibrium assumption in the calculations, the equation (15) is further simplified by using the following notations;

$$R_1 = k_1[O]_e[N_2]_e = k_{-1}[NO]_e[N]_e$$

Where, R$_1$ is the reaction rate using equilibrium concentrations for the reaction.
Similarly

$$R_2 = k_2[N]_e[O_2]_e = k_{-2}[NO]_e[O]_e$$

and

$$R_3 = k_3[N]_e[OH]_e = k_{-3}[NO]_e[H]_e$$

Using the above notations the equation (15) is simplified to give rate of formation of NO as below,

$$\frac{d[NO]}{dt} = \{2 \times R_1 \{1 - ([NO]/[NO]_e)^2\}/ \{1 + w[NO]/[NO]_e\} \qquad (16)$$

$$\text{Where,} \qquad w = R_1/\{R_2 + R_3\}$$

**Zone temperature**

A two-zone approach together with uniform pressure and the ideal gas law for each zone individually as well as for the complete combustion chamber allow computation of the each zone.
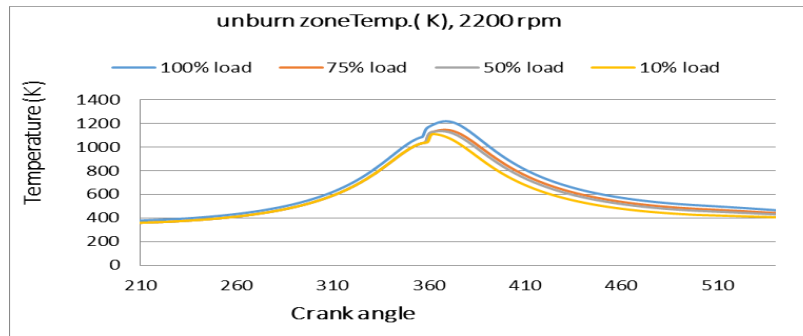


Figure 2:  Unburned zone temperature at 2200 rpm

Figure (2) shows the unburned zone temperature profile at 2200 rpm. The maximum temperature predicted at 100% load is 1218K at 368 degree CA while at 75% load, 50% load and 10% load are 1145K, 1135K, 1110K and their corresponding CA in degree are 368 degree CA, 365.5 degree CA and 362.5 degree CA respectively.  The unburned zone temperature profile essentially reflects the compression process, reaching its peak close to TDC, and dropping as the piston moves down. Due to higher inlet pressure and temperature at higher load the peak temperature is more in comparison with lower load as shown in figure 2.
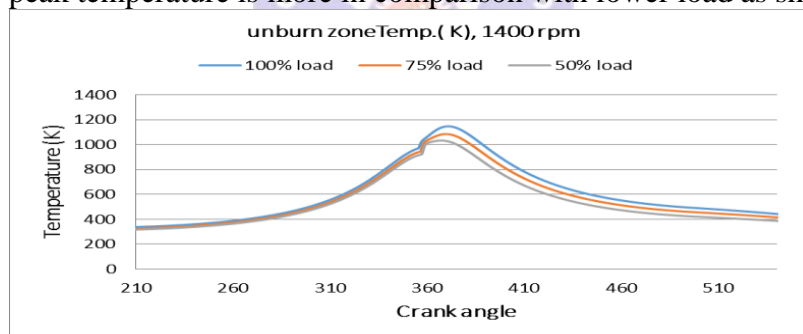


Figure 3:  Unburned zone temperature at 1400 rpm

If engine speed is lowered from 2200 rpm to 1400 rpm then the predicted peak temperatures at 100% load, 75% load and 50% load are 1147K, 1084K, 1033K and that time predicted crank angle in degree are 370 degree CA, 369 degree CA and 366.5 degree CA as shown in figure 3. This peak temperature mainly depend on inlet pressure and temperature condition which is already discussed in heat release section.
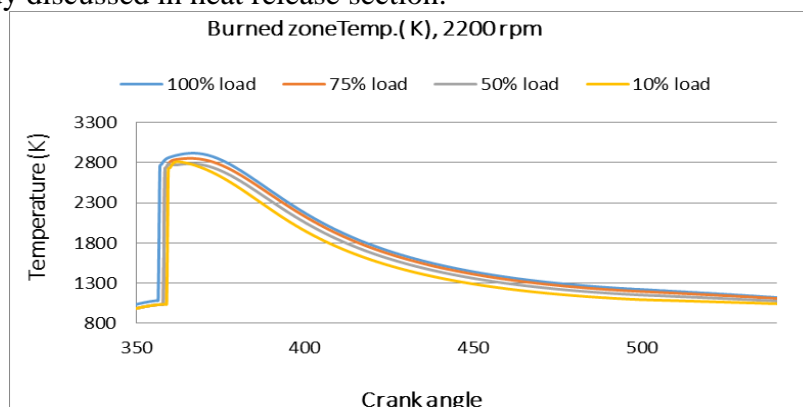


Figure 4:  Burned zone temperature at 2200 rpm

Burned zone temperature before considering flame temperature can be calculated using isentropic relationship as equation (25) and during combustion according to equation (26) of chapter-4. Figure 4 shows the burned zone temperature profile at 2200 rpm. The maximum

temperature predicted at 100% load is 1917K at 366.5 degree CA while at 75% load, 50% load and 10% load are 2853K, 2776K, 2811K and their corresponding CA in degree are 366 degree CA, 366 degree CA and 362 degree CA respectively

The burned zone temperature is very high near the TDC just after start of combustion and decreases as the expansion progresses.
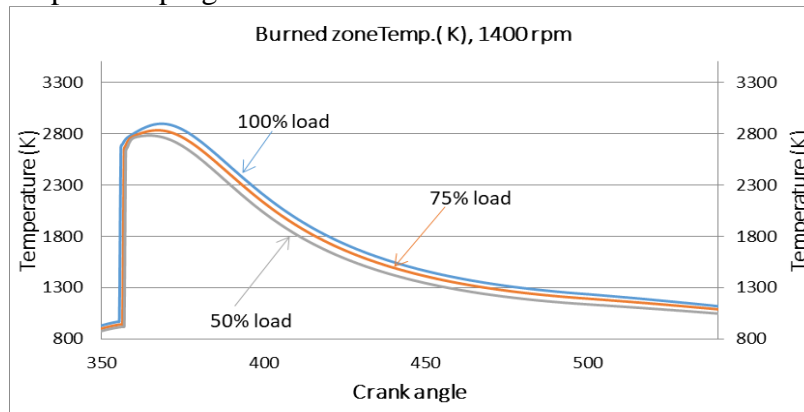


Figure 5: Burned zone temperature at 1400 rpm

If engine speed is lowered from 2200 rpm to 1400 rpm then the predicted burned zone peak temperatures are at 100% load, 75% load and 50% load are 2896K, 2833K, 2781K and that time predicted crank angle in degree are 369 degree CA, 367.5 degree CA and 365 degree CA. At higher load, more mass of fuel is injected in comparison to lower load condition and simultaneously higher pressure and temperature at SOC due to higher inlet pressure and temperature, results higher burned zone temperature.

The global or bulk cylinder temperature lies between the temperatures of burned zones and the air zone or unburned zone, and is considerably lower than the temperatures of burning or burned zone. Figure 4 and figure 5 shows the comparison of temperature profile between unburned, burned and global.
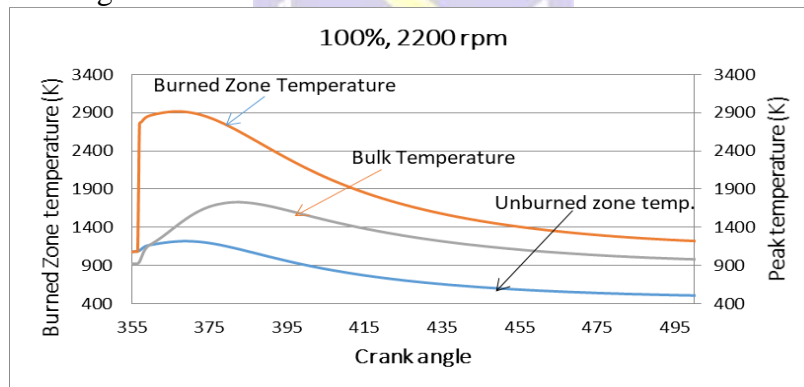


Figure 6: Comparison between unburned, burned and global temperature

At 100% load and 2200 rpm engine speed the peak temperature predicted is 1728K and corresponding crank angle is 382 degree CA, shown in figure 6.
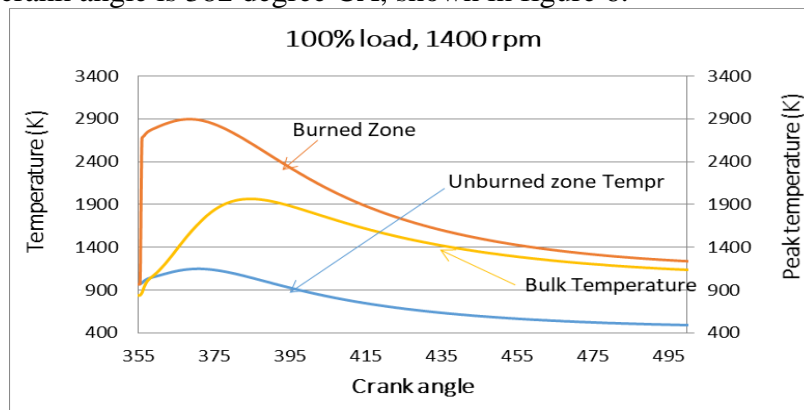


Figure 7: Comparison between unburned, burned and global temperature

Figure 7 shows the bulk temperature profile at 100% load and 1400 rpm. The maximum temperature predicted at 100% load is 1964K at 384.5 degree CA. The mean or global temperature is the average temperature of both unburned and burned zone temperature. Therefore, it always lies between both unburned and burned zone temperature.

**Equilibrium Concentration of species**

The equilibrium oxygen and nitrogen concentrations in the burned zone are functions of pressure and temperature [9]. All equilibrium concentrations were computed with an angular resolution of 0.5 CAD within each cycle, the resulting values are shown in figure (8), (9), and (10).
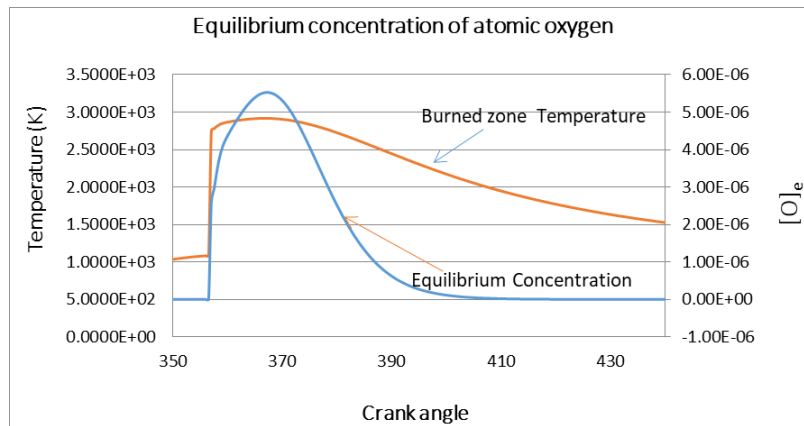


Figure 8: Equilibrium concentration of atomic oxygen at 2200 rpm and 100% load

The equilibrium concentration of atomic oxygen during combustion is varied throughout the cycle. The maximum concentration is 0.00000551 mol/cm$^3$ at 367 degree CA, when engine is running at a speed of 2200 rpm under full load, refer figure 5.28. Its value is directly proportional to burned zone temperature.
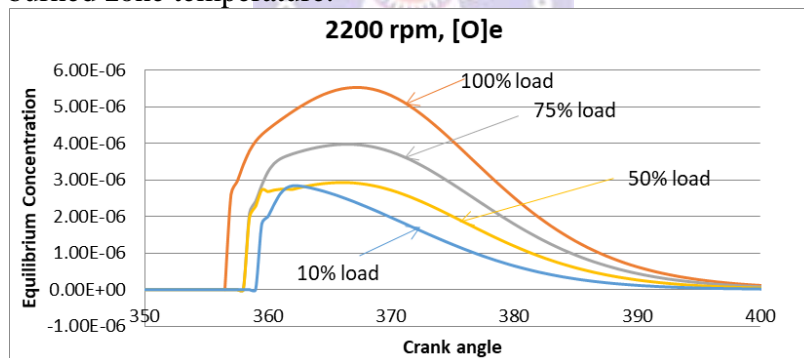


Figure 9 Comparison of equilibrium concentration of atomic oxygen at various load

As operating load on engine decreases from 100% to 10% at 2400 rpm as shown in figure 5.29, then concentration of atomic oxygen decreases due to decrease in burned zone temperature as already shown in figure 5.24.
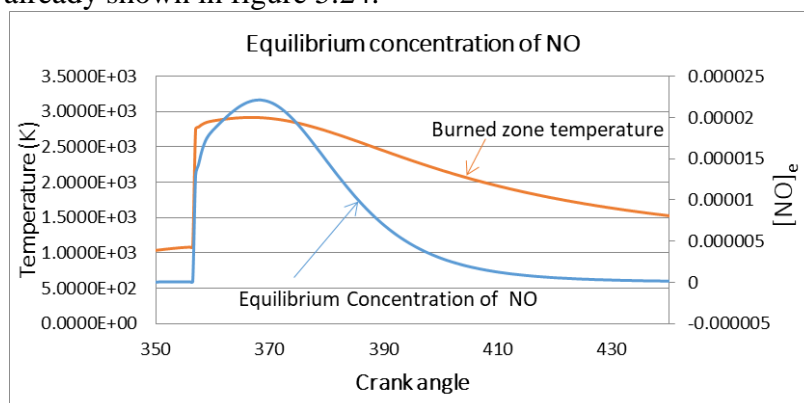


Figure 10: Equilibrium concentration of NO at 2200 rpm and 100% load

Figure 10 shows the equilibrium concentration of NO during combustion which is varied throughout the cycle with respect to burned zone temperature. Its maximum value is

0.000022124 mol/cm$^3$ at 368 degree CA when engine is running at a speed of 2200 rpm under full load. This maximum value occurs at maximum burned zone temperature.
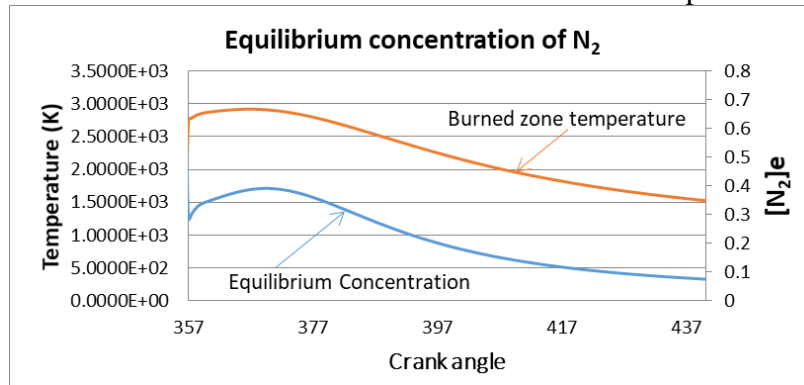


Figure 11: Equilibrium concentration of N$_2$ at 2200 rpm and 100% load

Similarly, Figure 11 shows the equilibrium concentration of NO during combustion which is also varied throughout the cycle with respect to burned zone temperature. Its maximum value is 0.3914 mol/cm$^3$ at 369.5 degree CA when engine is running at a speed of 2200 rpm under full load.

## Effect of engine load and rpm on engine NOx

Exhaustive study has been carried to analyse the effect of load on engine on NOx emission. A series of experiments have been carried out at different operating modes at engine speed of 2200 rpm and 1400 rpm. Figure 12 shows comparison between predicted and measured NOx Emission at different loads.
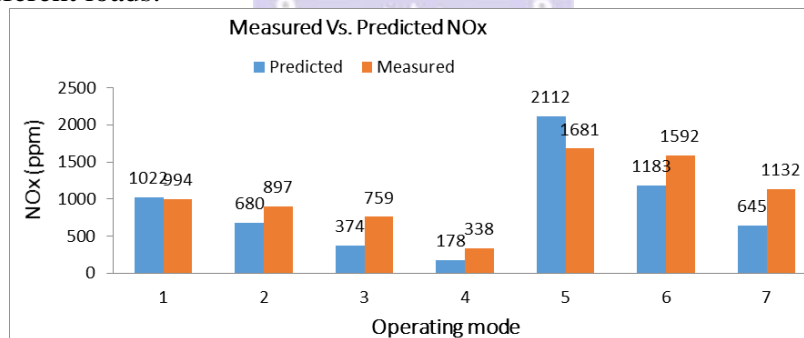


Figure 12: Comparison between measured vs. predicted NOx

Figure 12 shows operating points where the engine-out NOx level was above 100 ppm but accuracy was not so good. This was to be expected as only the Zeldovich mechanism was used to model NOx formation even though other mechanism are important at low temperatures .
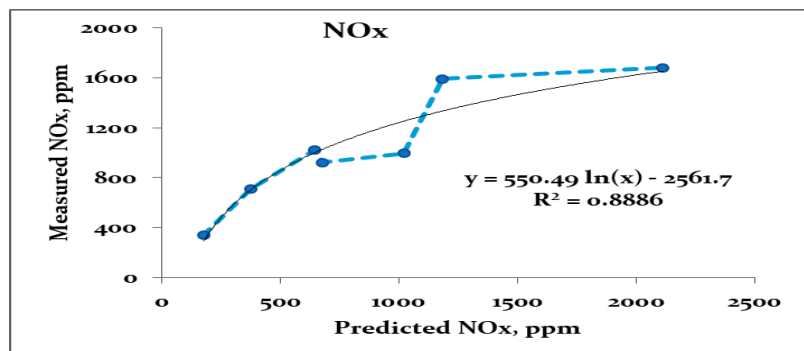


Figure 13. Curve-fit

However, if plotting measured NOx levels against model-out NOx using curve-fit, we got a simple mathematical equation as shown in figure 13.

This equation was then incorporated in the NOx model as an empirical correction algorithm, used at the end of each operating points. As the correction algorithm is purely empirical and based on the results from one engine only, there is no guarantee that this algorithm can be used in other engine. The resulting deviations in  NOx levels after curve fit at different operating points are listed in figure 14.
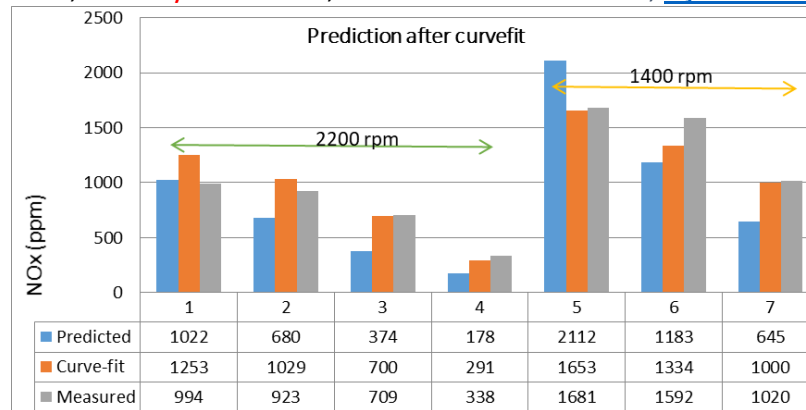
Figure 14: Prediction using curve-fit Equation

According to the figure 14 NOx seems to be over-predicted at higher engine load. One possible explanation for this might be that only the two reactions of the original Zeldovich mechanism are used. At low load, the influence of backward reactions consuming NO is greater than at higher load and the third reaction is an important contributor to the backward reaction.

## Conclusions

The NOx predicting model is developed with Précised accuracy for 4-stroke turbocharged DI diesel engine. In this work, different models were used for in-cylinder predictions along with NOx. The main findings of the work are summarised below:

- Higher the burned zone temperature higher the equilibrium concentrations of atomic oxygen, NO and nitrogen.
- After curve fit the predicted NOx data , the deviations observed at various operating modes i.e. full load, 75% load, 50% load and 10% load at 2200 rpm engine speed are -26.1%, -11.5%, 1.3% and 13.9% respectively. Similarly, at 1400 rpm, full load, 75% load, 50% load the deviations are 1.7%, 16.2%, and 2% respectively. We conclude that due to decrease in load at particular rpm (say 2200 rpm), NOx in ppm decreases but at lower engine speed (say 1400 rpm) and same operating load as used in 2200 rpm NOx in ppm increases

## References

[1] Agarwal, A.K., Shukla, P.C., Patel, C., Gupta, J.G., Sharma, N., Prasad, R.K. and Agarwal, R.A., 2016. Unregulated emissions and health risk potential from biodiesel (KB5, KB20) and methanol blend (M5) fuelled transportation diesel engines. Renewable Energy, 98, pp.283-291.

[2] Arrègle, J., López, J.J., Guardiola, C. and Monin, C., 2010. On board NOx prediction in diesel engines: a physical approach. In Automotive model predictive control (pp. 25-36). Springer, London.

[3] Moos, R., 2005. A brief overview on automotive exhaust gas sensors based on electroceramics. International Journal of Applied Ceramic Technology, 2(5), pp.401-413.

[4] Prasad, R.K. and Agarwal, A.K., 2021. Experimental evaluation of laser ignited hydrogen enriched compressed natural gas fueled supercharged engine. Fuel, 289, p.119788.

[5] Egnell, R., 1998. Combustion diagnostics by means of multizone heat release analysis and NO calculation. SAE transactions, pp.691-710.

[6] Timoney, D.J., Desantes, J.M., Hernández, L. and Lyons, C.M., 2005. The development of a semi-empirical model for rapid NO x concentration evaluation using measured in-cylinder pressure in diesel engines. Proceedings of the Institution of Mechanical Engineers, Part D: Journal of Automobile Engineering, 219(5), pp.621-631.

[7] Cipolat, D., 2007. Analysis of energy release and NOx emissions of a CI engine fuelled on diesel and DME. Applied Thermal Engineering, 27(11-12), pp.2095-2103.

[8] Hernández, J.J., Pérez-Collado, J. and Sanz-Argent, J., 2008. Role of the Chemical

Kinetics on Modeling NO x Emissions in Diesel Engines. Energy & fuels, 22(1), pp.262-272.

[9] Prasad, R.K., Mustafi, N. and Agarwal, A.K., 2020. Effect of spark timing on laser ignition and spark ignition modes in a hydrogen enriched compressed natural gas fuelled engine. Fuel, 276, p.118071.

[10] Del Re, L., Allgöwer, F., Glielmo, L., Guardiola, C. and Kolmanovsky, I. eds., 2010. Automotive model predictive control: models, methods and applications (Vol. 402). Springer.

[11] Andersson, M., Johansson, B., Hultqvist, A. and Noehre, C., 2006. A predictive real time NOx model for conventional and partially premixed diesel combustion. SAE Transactions, pp.863-872.

[12] Arrègle, J., López, J.J., Guardiola, C. and Monin, C., 2008. Sensitivity study of a NOx estimation model for on-board applications (No. 2008-01-0640). SAE Technical Paper.

[13] Desantes, J.M., Galindo, J., Guardiola, C. and Dolz, V., 2010. Air mass flow estimation in turbocharged diesel engines from in-cylinder pressure measurement. Experimental Thermal and Fluid Science, 34(1), pp.37-47.

[14] Luján, J.M., Bermúdez, V., Guardiola, C. and Abbad, A., 2010. A methodology for combustion detection in diesel engines through in-cylinder pressure derivative signal. Mechanical systems and signal processing, 24(7), pp.2261-2275.

[15] Leonhardt, S., Muller, N. and Isermann, R., 1999. Methods for engine supervision and control based on cylinder pressure information. IEEE/ASME transactions on mechatronics, 4(3), pp.235-245.

[16] Hasegawa, M., Shimasaki, Y., Yamaguchi, S., Kobayashi, M., Sakamoto, H., Kitayama, N. and Kanda, T., 2006. Study on ignition timing control for diesel engines using in-cylinder pressure sensor (No. 2006-01-0180). SAE Technical Paper.

[17] Shimasaki, Y., Kobayashi, M., Sakamoto, H., Ueno, M., Hasegawa, M., Yamaguchi, S. and Suzuki, T., 2004. Study on engine management system using in-cylinder pressure sensor integrated with spark plug (No. 2004-01-0519). SAE Technical Paper.

[18] Payri, F., Broatch, A., Tormos, B. and Marant, V., 2005. New methodology for in-cylinder pressure analysis in direct injection diesel engines—application to combustion noise. Measurement Science and Technology, 16(2), p.540.

[19] Hountals, D.T., Savva, N. and Papagiannakis, R.G., 2010. Development of a new physically based semi-empirical NOx model using the measured cylinder pressure. In Proceedings of the THIESEL Conference on Thermo-and Fluid Dynamic Processes in Diesel Engines. CMT.

[20] Devarakonda, M., Parker, G., Johnson, J.H. and Strots, V., 2009. Model-based control system design in a urea-SCR aftertreatment system based on NH 3 sensor feedback. International Journal of Automotive Technology, 10(6), p.653.

[21] Katare, S.R., Patterson, J.E. and Laing, P.M., 2007. Diesel aftertreatment modeling: A systems approach to NO x control. Industrial & engineering chemistry research, 46(8), pp.2445-2454.

[22] R. Stone, "Introduction to internal combustion engines". London: Macmillan; 1999 Nov 11.

[23] Johansson, B., Wilhelmsson, C., Tunestål, P., Johansson, R., & Widd, A. 2009. A Physical Two-Zone NOx Model Intended for Embedded Implementation. In SAE World Congress, 2009. SAE.

[24] Arsie, I., Di Genova, F., Pianese, C., Sorrentino, M., Rizzo, G., Caraceni, A., ... & Flauti, G. 2004. Development and identification of phenomenological models for combustion and emissions of common-rail multi-jet diesel engines (No. 2004-01-1877). SAE Technical Paper.

[25] Rakopoulos, C.D., Dimaratos, A.M., Giakoumis, E.G. and Rakopoulos, D.C., 2009. Exhaust emissions estimation during transient turbocharged diesel engine operation using a two-zone combustion model. International Journal of Vehicle Design, 49(1-3), pp.125-149